

Article

Study on Gaseous Chlorobenzene Treatment by a Bio-Trickling Filter: Degradation Mechanism and Microbial Community

Nan Liu ¹, Jia-Lin Lv ¹, Ya-Lan Cai ¹, Yan-Yan Yao ¹, Ke Zhang ¹, Chuang Ma ¹, Ji-Xiang Li ^{2,3}, Xiang-Yu Ren ^{4,*}, Jia-Jun Hu ⁵ and Ji-Hong Zhao ⁶

- ¹ Collaborative Innovation Center of Environmental Pollution Control and Ecological Restoration, Henan Province, Department of Material and Chemical Engineering, Zhengzhou University of Light Industry, Zhengzhou 450001, China; lnan2008@zju.edu.cn (N.L.); lj1923378@163.com (J.-L.L.); caiyalan0507@163.com (Y.-L.C.); yaoyanyan1998@163.com (Y.-Y.Y.); zkecolony@163.com (K.Z.); machuang@zzuli.edu.cn (C.M.)
- ² Shanghai Advanced Research Institute, Chinese Academy of Sciences, Shanghai 200120, China; lijixiang@sari.ac.cn
- ³ University of Chinese Academy of Sciences, Beijing 100049, China
- ⁴ Zhejiang Environment Technology Co., Ltd., Hangzhou 310000, China
- ⁵ Shanghai Key Laboratory of Bio-Energy Crops, School of Life Sciences, Shanghai University, Shanghai 200444, China; hujiajunsu@shu.edu.cn
- ⁶ Henan Radio & Television University, Zhengzhou 450001, China; zjh@zju.edu.cn
- * Correspondence: rxybxl@126.com

Abstract: Large-flow waste gas generated from the pharmaceutical and chemical industry usually contains low concentrations of VOCs (volatile organic compounds), and it is also the key factor that presents challenges in terms of disposal. To date, due to the limitations of mass transfer rate and microbial degradation ability, the degradation performance of VOCs using the biological method has not been ideal. Therefore, in this study, the sludge from a chlorobenzene-containing wastewater treatment plant was inoculated into our experimental bio-trickling filter (BTF) to explore the feasibility of domestication and degradation of gaseous chlorobenzene by highly active microorganisms. The kinetics of its mass transfer reaction and microbial community dynamics were also discussed. Moreover, the main process parameters of BTF for chlorobenzene degradation were optimized. The results showed that the degradation effect of chlorobenzene reached more than 85% at an inlet concentration of chlorobenzene 700 mg·m⁻³, oxygen concentration of 10%, and an empty bed retention time (EBRT) of 80 s. The mass transfer kinetic analysis indicated that the process of chlorobenzene degradation in the BTF occurred between the zero-stage reaction and the first-stage reaction. This BTF contributed significantly to the biodegradability of chlorobenzene, overcoming the limitation of gas-to-liquid/solid mass transfer of chlorobenzene. The analysis of the species diversity showed that *Thermomonas*, *Petrimona*, *Comana*, and *Ottowia* were typical organic-matter-degrading bacteria that degraded chlorobenzene efficiently with xylene present.

Keywords: chlorobenzene; bio-trickling filter; mass transfer kinetics; microbial communities; pharmaceutical and chemical industry



Citation: Liu, N.; Lv, J.-L.; Cai, Y.-L.; Yao, Y.-Y.; Zhang, K.; Ma, C.; Li, J.-X.; Ren, X.-Y.; Hu, J.-J.; Zhao, J.-H. Study on Gaseous Chlorobenzene Treatment by a Bio-Trickling Filter: Degradation Mechanism and Microbial Community. *Processes* **2022**, *10*, 1483. <https://doi.org/10.3390/pr10081483>

Academic Editors: Wei Li and Yinfeng Xia

Received: 7 June 2022

Accepted: 22 July 2022

Published: 28 July 2022

Publisher's Note: MDPI stays neutral with regard to jurisdictional claims in published maps and institutional affiliations.



Copyright: © 2022 by the authors. Licensee MDPI, Basel, Switzerland. This article is an open access article distributed under the terms and conditions of the Creative Commons Attribution (CC BY) license (<https://creativecommons.org/licenses/by/4.0/>).

1. Introduction

Volatile organic compounds (VOCs) with complex components are currently the main pollutants that affect air quality. VOCs not only play an important role in the formation of ozone and PM_{2.5}, but also cause great harm to human health. According to the announcement of the Second National Pollution Source Survey by the Ministry of Ecology and Environment of the People's Republic of China, 4.82 million tons of VOCs were emitted in 2017, with the pharmaceutical and chemical industry accounting for 23% of total volatile organic emissions. The air pollutants emitted from the pharmaceutical and chemical industries are mainly volatile organic compounds. Moreover, there are problems

such as large emissions, complex emission links, and high treatment costs [1]. In 2017, The Ministry of Ecology and Environment issued the “Plan for Prevention and Control of Volatile Organic Compounds during 2021–2025”, which required the chemical industry, including 7100 pharmaceutical companies and 2000 pesticide companies in China, to reduce VOC emissions by more than 30%.

Chlorinated volatile organic compounds (CVOCs) are highly toxic by-products that are difficult to degrade and complex in their formation [2]. Chlorobenzene is a typical representative of CVOCs and aromatic hydrocarbon compounds, and is often used as organic solvent in the chemical industry. The removal of chlorobenzene is currently difficult in the field of air pollution control. At present, the technologies for CVOC treatment include two main types of recycling and direct degradation. It is reported that low concentrations of organic pollutants ($<1000 \text{ mg}\cdot\text{m}^{-3}$) in the pharmaceutical and chemical industries are mainly degraded directly. Combustion produces dioxins that are toxic and difficult to degrade. The plasma cannot achieve high VOC removal efficiency, but readily releases secondary pollutants, such as ozone. However, the biological treatment process is a method in which microorganisms can utilize VOCs as carbon source and energy, therefore degrading VOCs through their own metabolism [3,4]. Compared with other technologies, it has the potential advantage of saving energy, and is especially suitable for dealing with the low concentrations of VOCs in exhaust gas. Thus, the biological treatment process can solve the problems of low degradation efficiency and the risk of by-products of the existing VOCs treatment technologies for the pharmaceutical and chemical industries. The bio-trickling filter (BTF) was introduced for the removal of odorous gases and soluble volatile organic compounds from exhaust gas in the mid-1980s. Coutu et al. found that the biological method achieved a removal efficiency of 69% with 1,2-dichlorobenzene [5]. Rahul et al. found that the maximum BTEX (benzene, toluene, ethylbenzene, and xylene) removal rate reached 99.85% when corn-cob was used with an inlet BTEX concentration of $97 \text{ mg}\cdot\text{m}^{-3}$ and an EHRT (equilibrium hydraulic retention time) of 3.06 min [6]. Compared with other reported methods of VOC removal, the biological method has more advantages in dealing with low concentrations of VOCs and high volumes of exhaust gas. However, the solubility of VOCs in the liquid phase is limited (the solubility of VOCs in water is no more than 5% in general), which has a negative influence on VOC removal from exhaust gas. Some studies improved the mass transfer of pollutants during the gas–liquid phase by changing the type of packing and the rate of liquid recirculation [7]. It was reported that good performance was obtained by introducing PDMS (polydimethylsiloxane) hydrophobic coating and adjusting the flow rate [8], so that the efficiency of removal of toluene reached more than 90% after a 3-day operation. In addition, some studies showed that surfactant also improved the treatment efficiency of hydrophobic chlorobenzene [9,10]. Moreover, few studies have improved the degradation performance of hydrophobic VOCs in BTF by optimizing bacterial strains [11]. Zhang et al. isolated and identified a new strain, *Mycobacterium Cosmeticum Byf-4*, which can simultaneously degrade BTEX compounds [12]. Compared with bacteria, fungi are more suitable for treating hydrophobic VOCs because of the advantages of aerial hyphae [13]. The *Cladophialophora* fungus has proved to be effective in degrading toluene to carbon dioxide completely [14]. However, since the metabolic rate of fungi is generally lower than that of bacteria, there is the problem that BTF, which is dominated by fungi, would require a long period for starting up. Furthermore, multi-component VOCs usually perform unpredictably in the biological degradation process [15]. Zhang et al. found that the carbon recovery in multi-substrate exceeded 91%, while the values of carbon recovery in other multi-substrate compositions containing o-xylene ranged from 79–81% [12]. O-xylene was found to have negative effect, but the microbial diversity had a better performance with mixed carbon sources. Due to the complex multiphase flow and multi-scale characteristics of BTFs, the mass transfer and biodegradation kinetics of BTFs are still unclear. A large number of simulation experiments have been conducted to study gas–liquid–biomass transfer in BTFs [4,16,17]. Moreover, Yang et al. found that the structure of the microbial communities changed with the differences in VOC components, which also determined

the degradation performance of the BTF [18]. Thus, the high-efficiency degrading strains are vital for the stability of BTFs and removal performance. In particular, high-throughput sequencing allows rapid, detailed, and comprehensive analysis of the transcriptome and genome of a species or microbial community. A number of microorganisms have shown degradation activities on chlorobenzene, such as *Shewanella decolorationis* S12 [19], *Ralstonia pickettii* L2 [20], *Escherichia hermannii* [21], and *Microbacterium* [22]. It was reported that the addition of xylene as another kind of carbon source was proved to increase the removal rate of CS₂ by high-throughput sequencing method [23]. Therefore, it is of great significance to improve the key process parameters of mass transfer affecting the degradation performance of VOCs.

The objective of this study is to evaluate the crucial process parameters of mass transfer in the removal of chlorobenzene from the exhaust gas of the pharmaceutical and chemical industries. A BTF was designed and inoculated with sludge from the sewage treatment plant of a pharmaceutical factory in Henan province, CHN. The biochemical reaction kinetics were explored to further optimized and gain insight into these processes of chlorobenzene removal from exhaust gas with low investment and operating costs.

2. Materials and Methods

2.1. Materials

Chlorobenzene (AR) and xylene (AR) were obtained from Zhengzhou PAINI Chemical Reagent of Chemistry Co., China. The basal medium was made up of the following compositions (per liter): 0.04 g·L⁻¹ Zn²⁺, 0.004 g·L⁻¹ Cu²⁺, 100 g·L⁻¹ NH₄⁺, 0.02 g·L⁻¹ Ca²⁺, 0.008 g·L⁻¹ Co²⁺, 0.002 g·L⁻¹ Mn²⁺, 32 g·L⁻¹ HPO₄²⁻, 16 g·L⁻¹ H₂PO₄⁻ [24]. All reagents were of analytical reagent grade. The gases (O₂ (99.999%), N₂ (99.999%), CO₂ (99.999%)) were supplied by Zhengzhou Yuan-Zhen Gas Products Co., Zhengzhou, China. Oxygen-free distilled water was used throughout the experiments.

2.2. Apparatus

The schematic diagram of the apparatus is shown in Figure 1. The gases were generated and controlled by gas cylinders (1–3), mixing tank, and mass flowmeter (4), (25 °C, 101.325 kPa), and the total flow was 2 L·min⁻¹. The volume fractions of N₂, O₂, and CO₂ were 89.96%, 10%, and 0.04%. Chlorobenzene (8) was placed in a water bath at 35 °C, and the total concentration of chlorobenzene and xylene was no more than 800 mg·m⁻³ before mixing. During the 3–4 weeks of the experiment, a fluctuation of ±4% was detected when a certain concentration of chlorobenzene was set. The four layers of the cylindrical BTF (10) were made of a polymethylmethacrylate (PMMA) column (total volume/height/diameter: 4 L/0.8 m/79.8 mm) (10), and a degassed desiccator was set on top of the BTF to eliminate the effect of water vapors on the gas flow rate. Some raschig-ring fillers (Φ10 × 10, about 2400 m²·m⁻³ in total specific surface area) were filled up to half of the reactor volume, and were regularly packed in the reactor. A tank (11) for liquid storage was set up at the bottom of the BTF. The inlet and outlet of liquid flow were controlled by a circulating pump (6) and the circulating flow rate was maintained at 5.17 m³·m⁻²·h⁻¹ at room temperature. Gas detection was mainly accomplished online by gas chromatography (12).

2.3. The Method of Biofilm Formation in the BTF

In this study, chlorobenzene was added as the sole carbon source to culture the biofilm accelerated by the method of rapid mud discharge domestication [25]; that is, the activated sludge was cultivated over a three-day period, then transferred into the BTF after removing the supernatant. This method was able to quickly remove the non-related bacteria and harmful substances of the original inoculated sewage, which was derived from the sewage treatment plant of a pharmaceutical factory in the Henan province, CHN.

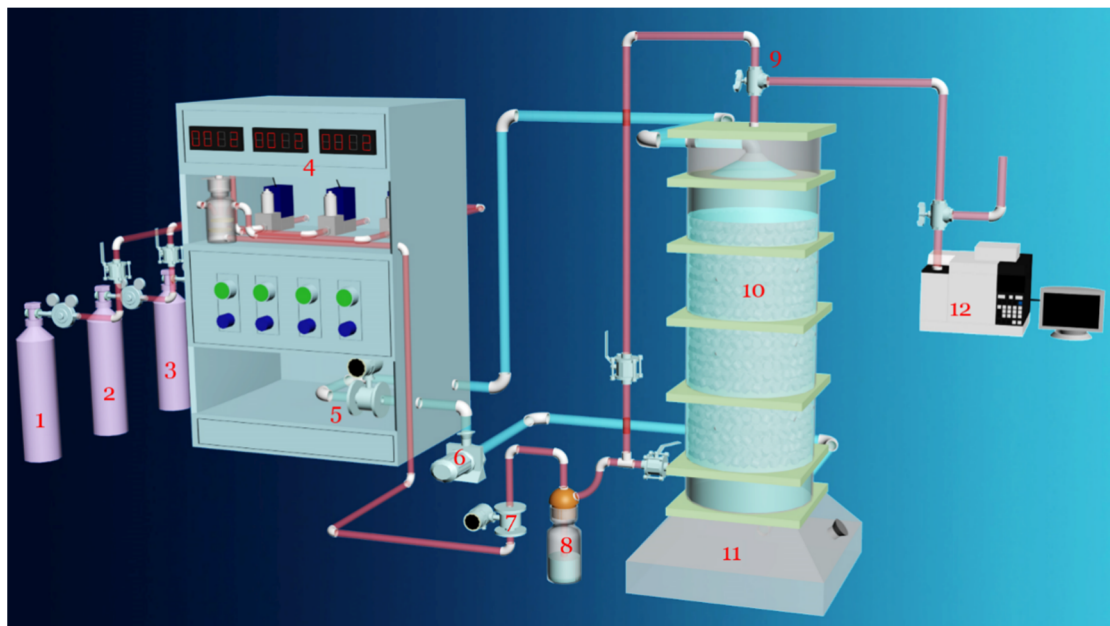


Figure 1. Schematic diagram of the bio-trickling filter: 1. N₂; 2. O₂; 3. CO₂; 4. Gas flowmeter; 5. Fluid flowmeter; 6. Circulating water pump; 7. Gas flowmeter; 8. Chlorobenzene; 9. Valve; 10. BTF; 11. Water tank; 12. Gas chromatography.

2.4. Study of Key Factors for Chlorobenzene Removal

The experiments were designed to investigate the removal of chlorobenzene under different initial chlorobenzene concentrations. The medium was replaced in the reactor every day. The chlorobenzene-degrading bacteria were cultured and gradually attached to the raschig-ring fillers. The influences of inlet degradation loadings on the biological activities in the BTF were observed by adjusting the concentrations of inlet chlorobenzene. The EBRT (empty bed retention time) of exhaust gas in BTF was changed by adjusting the rates of inlet flow gas. The interactions between the multiple organic components were explored by adding xylene.

Samples were taken at regular intervals for the measurement of the inlet and outlet concentrations of chlorobenzene. The operation of the BTF was described and studied in terms of the chlorobenzene removal efficiency (η) and the removal loading (q_e), which were evaluated using the following equation.

$$\eta = \frac{C_{in} - C_{out}}{C_{in}} \times 100\% \quad (1)$$

$$q_e = \frac{3.6Q(C_{in} - C_{out})}{V} \quad (2)$$

where C_{in} , and C_{out} denote the inlet and outlet chlorobenzene concentrations ($\text{mg}\cdot\text{m}^{-3}$) in the gas phase, respectively. Q is the flue gas flow ($\text{m}^3\cdot\text{s}^{-1}$) and V is the volume of empty column of BTF (m^3).

2.5. Biological Kinetics and Biological Community Analysis

2.5.1. Analysis of Biological Kinetics

Since the reduction of chlorobenzene and xylene is a relatively stable process, the metabolic rates of the single-component and multi-component substrates were analyzed by Michaelis–Menten equation [26].

$$\mu = \frac{\mu_{max}[S]}{K_m + [S]} \quad (3)$$

$$\frac{1}{\mu} = \frac{K_m + [S]}{\mu_{\max}[S]} = \frac{K_m}{[S]} + \frac{1}{\mu_{\max}} \quad (4)$$

where K_m ($\text{g}\cdot\text{m}^{-3}$) is the apparent semi-saturation constant, $[S]$ ($\text{g}\cdot\text{m}^{-3}$), which represents the ratio of substrate concentration in the liquid/solid phase and that in the gas phase. μ ($\text{g}\cdot\text{m}^{-3}\cdot\text{s}^{-1}$) is the reduction rate, and μ_{\max} ($\text{g}\cdot\text{m}^{-3}\cdot\text{s}^{-1}$) is the maximum apparent generation rate. Equation (4) expresses the apparent kinetic parameters of the chlorobenzene reduction.

However, mass transfer in the biological phase is a key factor affecting the efficiency of removal of chlorobenzene in the BTF. It is reported that the rate of VOC mass transfer (R) per unit in a uniformly mixed liquid phase can be expressed as follows:

$$R = \frac{Q}{V_r} \beta_s^* (C_{in} - m_w C_w) = (C_{in} - C_{out})/t \quad (5)$$

where C_w ($\text{mg}\cdot\text{m}^{-3}$) is concentration of VOCs in the liquid/solid phase; V_r (m^3) is effective volume of reactor; m_w is Henry coefficient of VOCs in the liquid phase (water); t (h) is time; β_s^* is the maximum fraction of VOCs from the gas phase to the liquid phase (water), and the β_s^* should be equal to 1 (dimensionless) in an idealized BTF. The β_s^* can be obtained as follows [27,28]:

$$\beta_s^* = \frac{C_{in} - C_{out}}{C_{in} - m_w C_w} \quad (6)$$

Furthermore, macro-kinetic biodegradation was also discussed. The degradation of VOCs by BTF can be regarded as a combined process of mass transfer and biodegradation. The transport and diffusion of VOCs occurs in the gas phase, while the process of biodegradation occurs in the liquid film and biofilm [26]. Based on the experimental results and theoretical analysis, the amount of oxygen consumption by microorganism was only 3% in total, that is, the oxygen was supplied in excess. Therefore, the O_2 concentration in the gas phase can be regarded as constant. The material balance of VOCs in the liquid/solid phase of the BTF is described as follows:

$$\frac{\partial C_w}{\partial t} = K(C_w^* - C_w) - bC_w^* \quad (7)$$

where b is the biodegradation rate constant; n is the order of reaction; K (h^{-1}) is the transfer coefficient; C_w^* ($\text{mg}\cdot\text{m}^{-3}$) is the Concentration of contaminants in the liquid/solid phase at equilibrium.

2.5.2. Analysis of Biological Community

Microbial samples were collected from the biofilm during the period of biofilm formation and steady stage. Metagenomics analysis was performed by 16S rDNA high-throughput sequencing [29]. The main steps were as follows: Sample preparation → DNA extraction → PCR amplification → Gene library preparation and detection → Miseq sequencing [30]. The sequencing data were processed by obtaining a valid sequence for cluster analysis after the removal of the chimeric sequence, and the representative sequence of each cluster was determined within the species distribution of each sample by taxonomic analysis [31]. The diversity of species was analyzed based on the results of ACE, Chao1, and Shannon index, and the community structure was analyzed at each classification level based on taxonomic information.

2.6. Analytical Methods

The concentrations of chlorobenzene and xylene were both determined by gas chromatography (Agilent 7820A, Palo Alto, CA, USA, HP-Innowax, column temperature 160 °C). A field environmental scan electron Microscope (FESEM, Philips Model XL30, Eindhoven, The Netherlands) was used to observe the formed biofilm and the surface of the fillers. All data shown in this paper were the mean values of duplicate or triplicate

experiments were analyzed by Origin 8.0. Confidence level used in this article was 95%, while probability of different results was determined by t-distribution.

3. Results and Discussion

3.1. Biofilm Formation in the BTF

Batch experiments were conducted with a solution containing the ratio of chlorobenzene and glucose 1:1 for the startup of the BTF. After 600 h cultivation, the degradation efficiency of chlorobenzene stabilized to about 70% (Figure 2) under the maximum inlet concentration of chlorobenzene $1000 \text{ mg}\cdot\text{m}^{-3}$, and a biofilm became visible on the surface of the fillers.

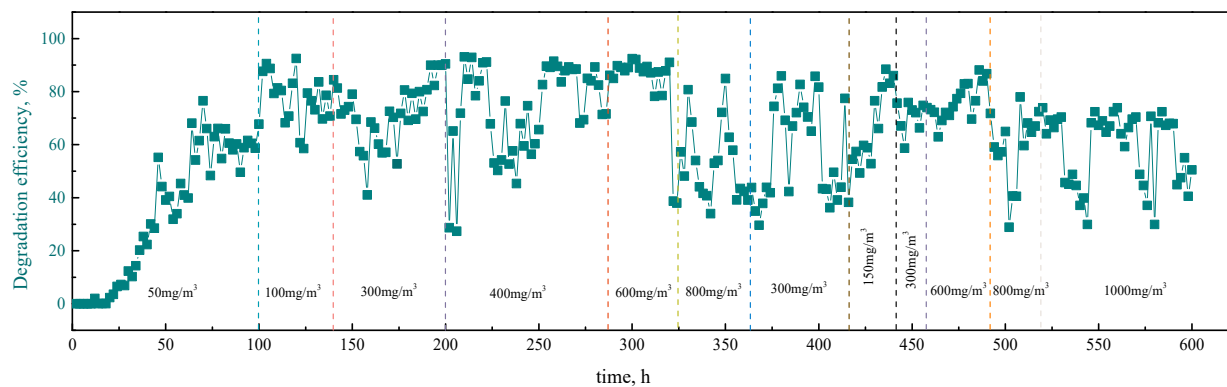


Figure 2. Reduction efficiency of chlorobenzene during biofilm formation. Inlet concentration of chlorobenzene = $50\text{--}1000 \text{ mg}\cdot\text{m}^{-3}$, liquid rate = $5.17 \text{ m}^3\cdot\text{m}^{-2}\cdot\text{h}^{-1}$, EBRT = 96 s, pH = 6.5–7.0, oxygen concentration = 10%. ■ Reduction efficiency of chlorobenzene.

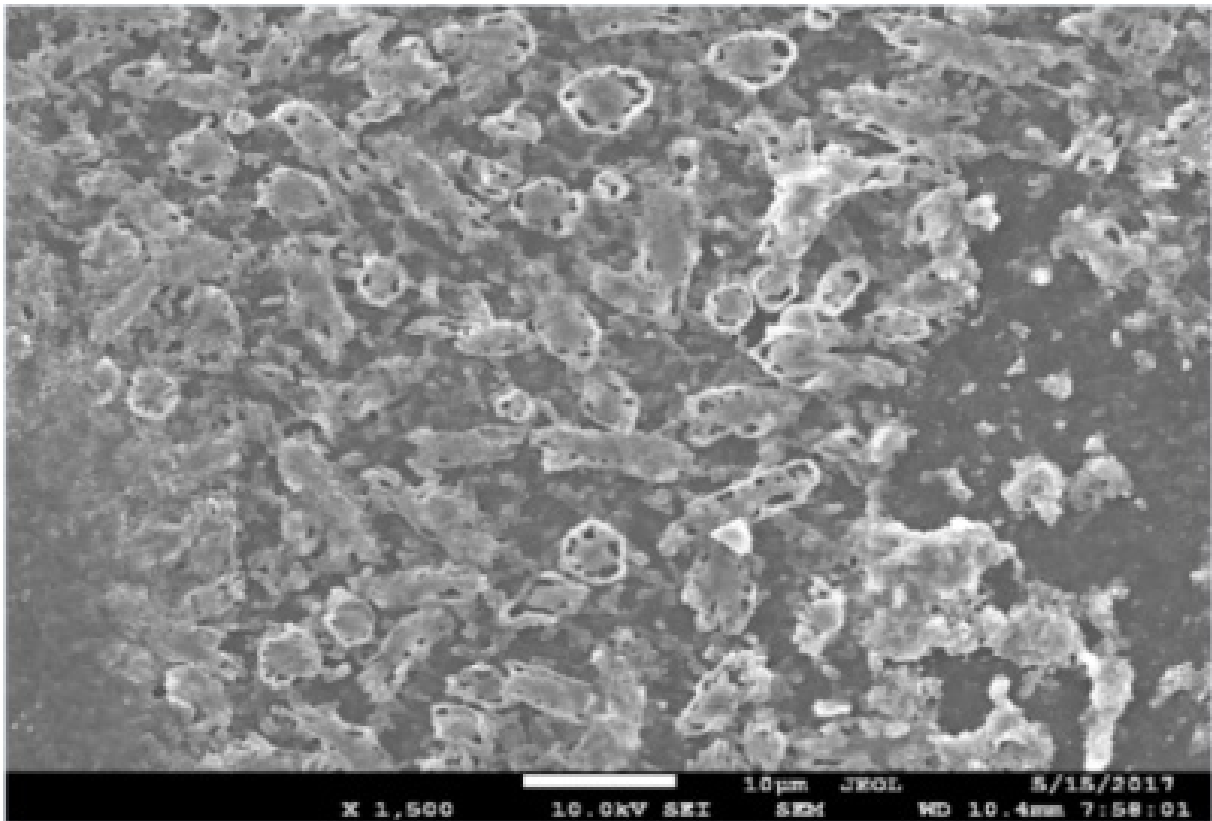
The biofilm had already formed, as shown in Figure 3. In this study, the volume load of chlorobenzene increased significantly at 25 d. Compared with the previous study [20], the loading of chlorobenzene was $700 \text{ mg}\cdot\text{m}^{-3}$ after 35 d. Therefore, a higher loading and more stability could be achieved by the method of rapid mud discharge in a short time.

Further, we can see from Figure 3 that the biofilm on the lower fillers was much thicker than that on the upper ones after 600 h operation. The reason is that the upper fillers were suffered by the spraying impulse damaged by the spraying. On the other hand, the biofilm was mainly made by the kinds of aerobic microorganisms, while the microorganisms on the lower fillers were more likely to maintain the activities by using oxygen passed through from the bottom of the biofilter.

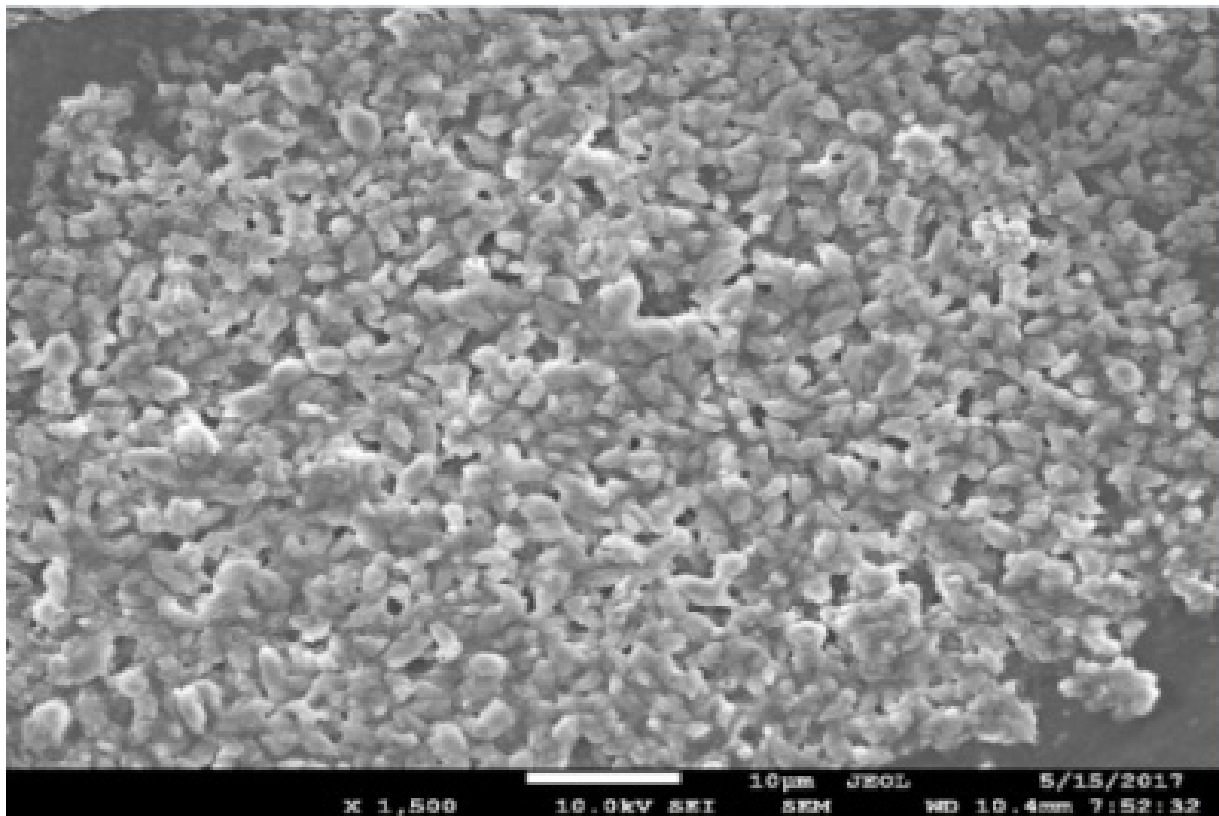
3.2. Optimization of the Operating Parameters of the BTF

3.2.1. Influence of Inlet Concentration of Chlorobenzene

The effect of inlet concentration of chlorobenzene on the operation of the BTF is shown in Figure 4. When the inlet concentration of chlorobenzene was raised from $50 \text{ mg}\cdot\text{m}^{-3}$ to $300 \text{ mg}\cdot\text{m}^{-3}$, the available carbon source for microorganisms gradually increased, so the degradation of chlorobenzene was raised from 85% to 88%. It remained at about 78% when the inlet concentration of chlorobenzene was between $400\text{--}700 \text{ mg}\cdot\text{m}^{-3}$. Moreover, the degradation efficiency was maintained at 60% at $1500 \text{ mg}\cdot\text{m}^{-3}$. It can be deduced that the massive inlet concentration of chlorobenzene was toxic toward the activity of the bacteria, leading to a gradual decline in degradation efficiency. Padhi et al. also found a negative correlation between VOC concentration and degradation efficiency when treating organic waste gas with BTF [32]. This indicates that the inhibition of effective biomass and gas-liquid mass transfer occurred in the system under a high inlet loading of chlorobenzene, so the capacity of substrate conversion per volume of biomass was close to the maximum. If the loading of chlorobenzene further increased, the biological activity in the system was inhibited, and then the substrate conversion capacity also reduced.



(a)



(b)

Figure 3. (a) SEM image of biofilm at the top; (b) SEM image of biofilm at the bottom.

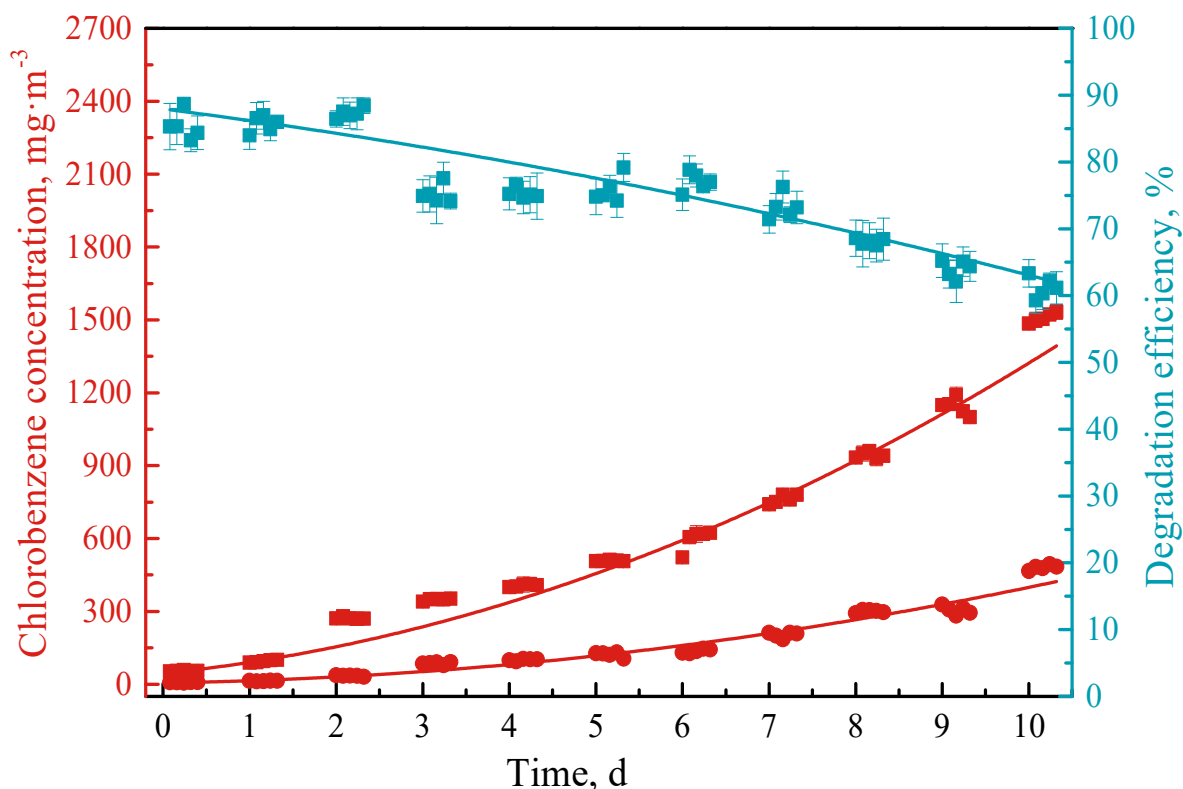


Figure 4. The degradation efficiency of chlorobenzene under different chlorobenzene concentrations. Liquid Rate = $5.17 \text{ m}^3 \cdot \text{m}^{-2} \cdot \text{h}^{-1}$, EBRT = 48 s, pH = 6.5–7.0, Oxygen Concentration = 10%. ■ Degradation efficiency ■ Inlet concentration ● Outlet concentration.

3.2.2. Influence of EBRT

The EBRT of simulated waste gas in the BTF has a great influence on the performance of chlorobenzene degradation [33–35]. The experiment analyzed the influence of different EBRT on the chlorobenzene degradation of the BTF; results are shown in Figure 5. With the EBRT increasing, the degradation of chlorobenzene showed a trend of increment. The maximum degradation reached 96% when the EBRT was 160 s. It also can be seen from Figure 5 that the removal loading improved with the increase in the EBRT. The removal loading reached $38 \text{ g} \cdot \text{m}^{-3} \cdot \text{h}^{-1}$ when the EBRT was 80 s. After the EBRT exceeded 80 s, there was no obvious impact on the removal loading, which remained at $40 \text{ g} \cdot \text{m}^{-3} \cdot \text{h}^{-1}$. This was due to the limitation of effective biomass and gas–liquid mass transfer in the system, and the capacity of substrate conversion per volume of biomass was close to the maximum. Li et al. found that the removal loading reached $35 \text{ g} \cdot \text{m}^{-3} \cdot \text{h}^{-1}$ with an inlet chlorobenzene concentration of $1670 \text{ mg} \cdot \text{m}^{-3}$ and an EBRT of 90 s, which was, however, lower than our result [36]. If the inlet concentration of chlorobenzene or the EBRT further increased, the microbial activity might be inhibited in the system. The degradation effect of chlorobenzene declined [37,38]. Therefore, an EBRT of no more than 80 s was determined to be sufficient in this system.

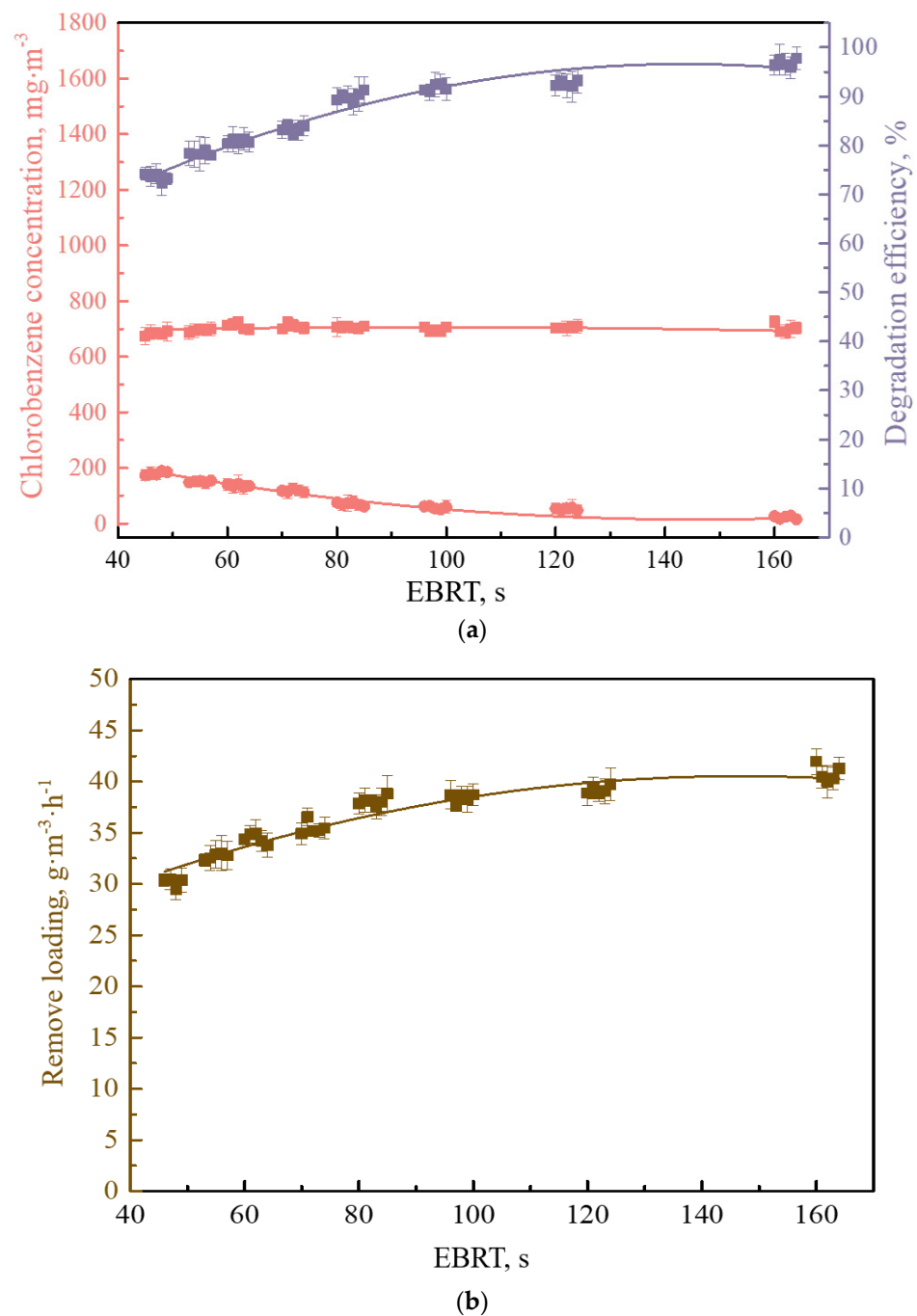


Figure 5. (a) The degradation efficiency of chlorobenzene under different EBRTs. (b) The removal loading of chlorobenzene under different EBRTs. Inlet concentration of chlorobenzene = $700 \text{ mg}\cdot\text{m}^{-3}$, liquid rate = $5.17 \text{ m}^3\cdot\text{m}^{-2}\cdot\text{h}^{-1}$, pH = 6.5–7.0, oxygen concentration = 10%. ■ Degradation efficiency ■ Inlet concentration ● Export concentration.

3.2.3. Influence of Xylene Concentration on Chlorobenzene Degradation

BTFs often deal with multi-component organic gas, and different organic compounds often inhibit each other in the biodegradation process. Therefore, it is of great significance to study the interaction between different organic compounds [23,39,40]. Figure 6 shows the degradation efficiencies of xylene and chlorobenzene at different concentration ratios. The degradation efficiencies of chlorobenzene were observed by changing different concentration ratios of chlorobenzene and xylene in organic waste gas. When the concentration ratio of chlorobenzene and xylene was 1:1, the degradation efficiencies of chlorobenzene

reached a maximum of 87.6%. The degradation efficiency is 14.1% higher than that of 14.1% result achieved with an inlet chlorobenzene concentration of $800 \text{ mg}\cdot\text{m}^{-3}$ in Figure 4. However, when the concentration ratio of chlorobenzene and xylene was 1:5 or 5:1, the average degradation efficiencies declined to 62.26% and 68.52%, respectively. Therefore, regardless of which organic compound had a higher concentration, the overall degradation efficiency was reduced, which may have been caused by the influence of the degradation pathway of chlorine and methyl groups on microorganism activities. Above all, the chlorobenzene and xylene both had a better removal efficiency under the ratio of 1:1.

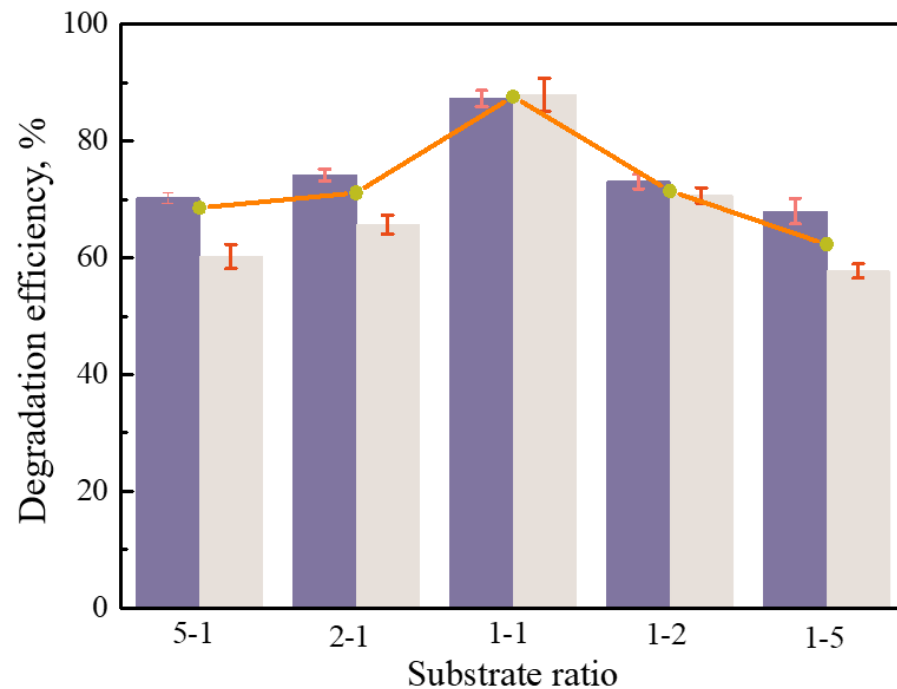


Figure 6. The degradation efficiency of chlorobenzene with different mixed waste gas concentrations. Inlet concentration of mixed waste gas = $800 \text{ mg}\cdot\text{m}^{-3}$, liquid rate = $5.17 \text{ m}^3\cdot\text{m}^{-2}\cdot\text{h}^{-1}$, pH = 6.5–7.0, oxygen concentration = 10%. ■ Xylene degradation efficiency ■ Chlorobenzene degradation efficiency.

3.3. Dynamics Analysis of Biodegradation

3.3.1. Kinetic Analysis of Enzymatic Reaction

In the process of biological treatment of organic waste gas, the mass transferred simultaneously with the degradation of organic waste gas by microorganisms. Organic waste was degraded by microorganisms mainly in the liquid film or biofilm [33]. Assuming that the oxygen is sufficient for the aerobic respiration of microorganisms, the degradation process of organic wastes and the activity of microorganism enzymes in the BTF can be expressed by the *Michaelis–Menten* equation.

$$\frac{1}{\mu} = \frac{K_m + [S]}{\mu_{max}[S]} = \frac{K_m}{\mu_{max}} \cdot \frac{1}{[S]} + \frac{1}{\mu_{max}} \quad (8)$$

Meanwhile, $[S]$ can be expressed as:

$$[S] = C_{in} \times \beta_s^* \quad (9)$$

The β_s^* value of chlorobenzene was determined and fitted by Formula (6). According to the results of this experiment, the β_s^* value reached 0.86, which was significantly increased compared with results from a traditional bioreactor. Therefore, it is speculated that this BTF reactor has a higher effect on gas-biomass transfer.

The relationships between $1/\mu$ and $1/[S]$ from the Michaelis–Menten equation are shown in Figure 7, respectively. The R^2 value is 0.97, indicating that this process can be well described by the *Michaelis–Menten* equation. When the carbon source was a substrate with a single component, the K_m values of chlorobenzene and xylene were $4.37 \text{ g}\cdot\text{m}^{-3}$ and $4.99 \text{ g}\cdot\text{m}^{-3}$, respectively. When the carbon source was a substrate with mixed components, the K_m values of chlorobenzene and xylene were $5.69 \text{ g}\cdot\text{m}^{-3}$ and $4.87 \text{ g}\cdot\text{m}^{-3}$, respectively. The physical meaning of K_m is similar to enzyme kinetics; that is, the higher of K_m value, the lower the affinity between pollutant and enzyme [41]. The K_m value of chlorobenzene under the mixed carbon source was higher than that of chlorobenzene as the sole carbon source. This means that the removal rate of chlorobenzene under the mixed carbon source was lower than that under the solo carbon source. K_m can also be regarded as a saturation constant of volume in the BTF. Zhou [20] et al. also studied the treatment of CB by BTF, and the results showed that the K_m value of the BTF system was $0.08 \text{ g}\cdot\text{m}^{-3}$, and with the BTF strengthened by *Ralstonia Pickettii* L2, the K_m value of the BTF system was $0.23 \text{ g}\cdot\text{m}^{-3}$. However, the K_m shown in this paper was much higher. However, we can draw the opposite conclusion regarding the removal rate of xylene due to the difference in the K_m values of xylene with mixed and single carbon sources. It can also be seen from Figure 6 that the removal rate of chlorobenzene was increasing, even though the K_m value of chlorobenzene under mixed carbon source was higher, because the inlet concentration of chlorobenzene decreased when xylene was added into the reactor. The removal rate of xylene also increased, since the K_m value of xylene under the mixed carbon source was lower, which is consistent with the conclusion obtained from the *Michaelis–Menten* equation. When the inlet concentrations of chlorobenzene and xylene were equal, better removal efficiency with both chlorobenzene and xylene was obtained. With the continuous increase in xylene, removal efficiency with both chlorobenzene and xylene decreased. A possible reason for this is that a large amount of xylene inhibited the activity of chlorobenzene-degrading bacteria, resulting in a decreased removal rate of chlorobenzene. In the meantime, the activity of xylene-degrading bacteria in the reactor was also insufficient to support the degradation of excess xylene.

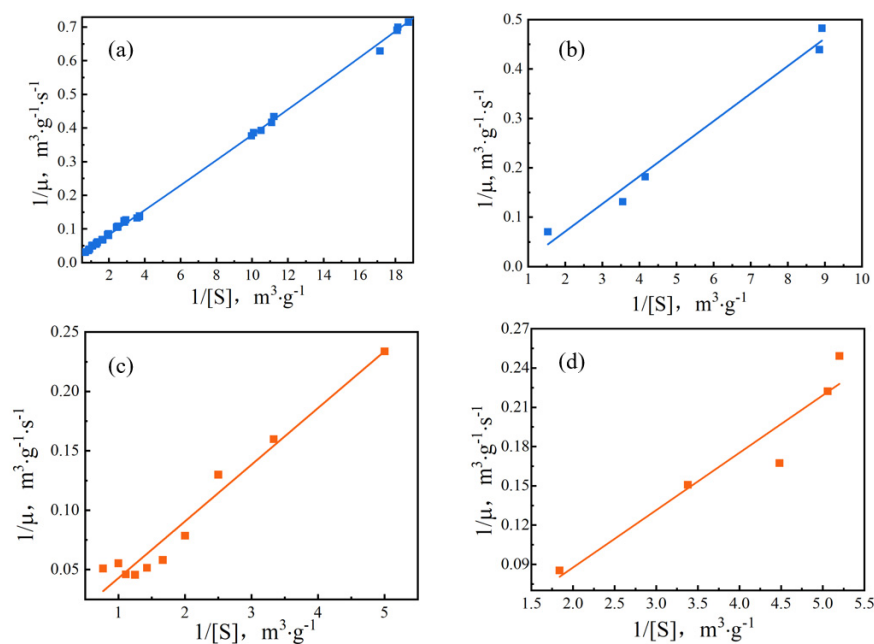


Figure 7. Kinetics of the biodegradation process. (a) Biodegradation of chlorobenzene; (b) biodegradation of chlorobenzene with mixed components substrate of chlorobenzene and xylene; (c) biodegradation of xylene; (d) biodegradation of xylene with mixed-component substrate of chlorobenzene and xylene.

In general, the K_m value also can reflect the reaction order [42]. It is speculated that when $[S]$ was less than $0.01 K_m$, $[S]$ was less than $0.044 \text{ g}\cdot\text{m}^{-3}$, and μ was equal to $(\mu_{max}/K_m)[S]$, the reaction was a kind of first-order reaction. The reaction rate was proportional to the substrate concentration. While $0.01 K_m < [S] < 100 K_m$, the substrate $[S]$ was between $0.044 \text{ g}\cdot\text{m}^{-3}$ to $437 \text{ g}\cdot\text{m}^{-3}$, and the reaction was between the zero-stage reaction and the first-stage reaction with the solo carbon source of chlorobenzene, which was consistent with the conclusion from Figure 4. When $[S]$ was more than $100 K_m$, μ was equal to μ_{max} . That is, while the substrate $[S]$ was over $437 \text{ g}\cdot\text{m}^{-3}$, the reaction rate was close to a constant value, and the enzyme was almost saturated with the substrate. The reaction rate had nothing to do with the concentration of substrates. It is recognized as a zero-order reaction, that is, $\frac{1}{\mu} = \frac{1}{\mu_{max}}$, $\mu \approx \mu_{max} = 116.28 \text{ g}\cdot\text{m}^{-3}\cdot\text{s}^{-1}$.

3.3.2. Macro-Dynamics Analysis of Biodegradation

The VOC transfer process is the main inflow, diffusion inflow, interphase transfer, and interphase transfer amount that will eventually be used by microorganisms. A micro element on the main flow direction can be selected and calculated by material balance, so a simplified model is obtained as follows:

$$\frac{\partial C}{\partial t} = D \frac{\partial^2 C}{\partial z^2} - v \frac{\partial C}{\partial t} - \left(\frac{1-\theta}{\theta} \right) K(C_w^* - C_w) \quad (10)$$

where C_w ($\text{mg}\cdot\text{m}^{-3}$) is concentration of VOCs in the gas-phase main body; D is axial diffusion coefficient in gas phase; z (m) is the effective height of reactor; θ is the porosity of raschig-ring fillers; v is the interstitial velocity. Thus, combined with Equations (7) and (10):

$$\frac{\partial C}{\partial t} = D \frac{\partial^2 C}{\partial z^2} - v \frac{\partial C}{\partial t} - \left(\frac{1-\theta}{\theta} \right) \left(\frac{\partial C_w}{\partial t} + bC_w^n \right) \quad (11)$$

when the system is in equilibrium, $C_w^* = K_h \times C_W$ and the situation of diffusion can be ignored. K_h is the ratio of the pollutant concentration in the liquid/solid phase and that in the gas phase, $K_W = K_h \times \left(\frac{1-\theta}{\theta} \right)$, K_W is the ratio of the pollutant mass in the liquid/solid phase and that in the gas phase. The range of v is 0 to inlet flow rate of VOCs. At the ideal status, $\frac{z}{v}$ can be deemed as $\frac{\pi r^2 \cdot z}{Q}$; that is, t_{EBRT} . Moreover, if the BTF kept stable, the boundary conditions of Equation (11) were $z = 0 \sim z$ and $C = C_{in} \sim C$. When the n is equal to 1 and 0, Equation (11) is integrated as follows:

$$\ln C_{in} - \ln C = bK_w t_{EBRT} \quad (12)$$

$$C_{in} - C = \frac{b}{\theta} (1-\theta) \cdot t_{EBRT} \quad (13)$$

where t_{EBRT} (s) is empty bed retention time. When the system was stable, the quantity of pollutants adsorbed by the biofilm was equal to the amount of biofilm biochemically removed. Therefore, according to the Langmuir adsorption formula, the reciprocal of the degree of adsorption of pollutants was linearly related to the reciprocal of the concentrations of pollutants. The intercept is expressed as the reciprocal of adsorption constant ($1/b$), so the parameter of b can be determined as 69.4 by experimental data. Taken into Equation (12) for fitting from Figure 8, R^2 value was 0.91, indicating that this process can be well described. K_W was calculated as 0.00034. The quantity of pollutants transferred into biofilm per unit time was small, so the K_W value was not ideal. However, the flow rate of chlorobenzene in the gas phase was $1.4 \text{ mg}\cdot\text{min}^{-1}$, while the microbial degradation rate reached up to $16.66 \text{ mg}\cdot\text{min}^{-1}$, which was much higher than the flow rate of chlorobenzene. Once the chlorobenzene was absorbed by the biofilm, it decomposed promptly. Thus, the C_{out} can be expressed as follows:

$$C_{out} = e^{-0.0237 t_{EBRT}} \cdot C_{in} \quad (14)$$

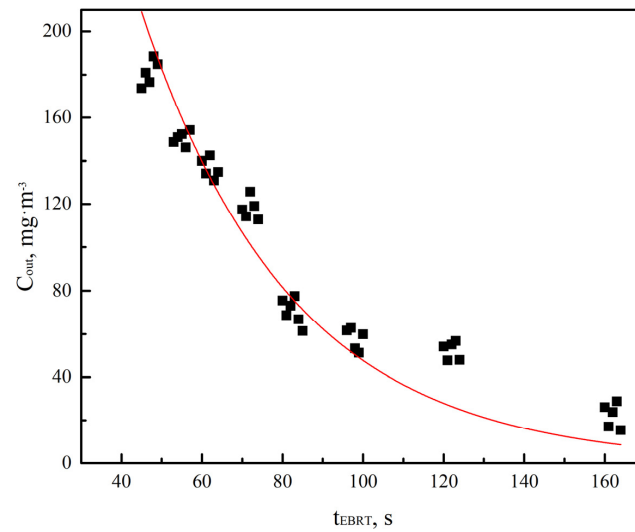


Figure 8. The relationship between outlet concentration of chlorobenzene and EBRT. (Liquid rate = $5.17 \text{ m}^3 \cdot \text{m}^{-2} \cdot \text{h}^{-1}$, pH = 6.5–7.0, oxygen concentration = 10%).

As is shown in Figure 5, the removal loading did not increase noticeably when the EBRT exceeded 80 s. The relationship between outlet concentration of chlorobenzene by biodegradation and time of long-term run under different inlet concentrations of chlorobenzene is shown in Figure 9, and it can be expressed as Formula (15).

$$\ln C_{in} - \ln C = bK_w t_R \quad (15)$$

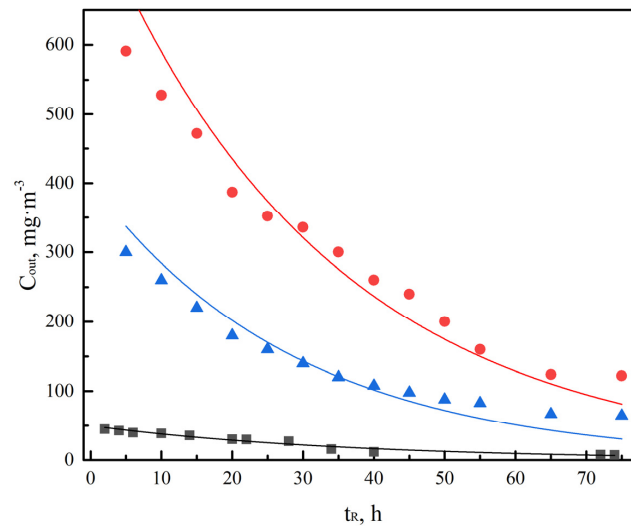


Figure 9. The relationship between outlet concentration of chlorobenzene and time of long-term run under different inlet concentrations of chlorobenzene. Liquid rate = $5.17 \text{ m}^3 \cdot \text{m}^{-2} \cdot \text{h}^{-1}$, pH = 6.5–7.0, oxygen concentration = 10%. ■ $100 \text{ mg} \cdot \text{m}^{-3}$ ▲ $400 \text{ mg} \cdot \text{m}^{-3}$ ● $800 \text{ mg} \cdot \text{m}^{-3}$.

These macro-dynamic models can satisfactorily predict the operation at different time scales, and both R^2 are beyond 0.92. With the increase in long-term run time, the values of adsorption constant (b) in the experiment remained stable, and the degradation capacity of biofilm was close to the maximum value. K_W was calculated as 0.00043; that is, almost the same as the value of K_W with different EBRTs. When the time of run increased, the activity of the biofilm was inhibited by VOC concentration, which is the same as the conclusion from Figure 5. Therefore, the process of chlorobenzene degradation was regarded as a first-stage reaction. Furthermore, when the t was less than 80 s, the degree of degradation

of the chlorobenzene was related to K_W . When the t was over 80 s, chlorobenzene was fully exposed to microorganisms.

3.4. Evaluation of the Microbial Communities in the BTF

In order to better understand the diversification of microbial communities and abundance characteristics of microorganisms under long-term operation of the BTF, high-throughput sequencing was utilized. Samples were collected at different operating steps. The conditions of collecting samples are shown in Table 1.

Table 1. Samples under different sampling conditions.

Seq.	Sample	Substrate
1	C-1	chlorobenzene as sole carbon source with the BTF operated stably
2	X-1	xylene as sole carbon source
3	C+X	chlorobenzene and xylene as mixed carbon source
4	C-2	chlorobenzene as sole carbon source maintained under acidic conditions

3.4.1. α -Diversification

α -diversification is a sign of species diversity, which can precisely reflect the number of species in a microbial community. The statistics of α -diversification are shown in Table 2. The total number of species are expressed as ACE and Chao indexes. The Shannon and Simpson indexes reflect the diversity and distribution of microbial species; the Coverage index represents the coverage rate. All the coverage values in the table are 1, indicating that the sample could be well detected.

Table 2. Statistics of α -diversification of species.

Sample	ACE	Chao	Shannon	Simpson	Good's Coverage
C-1	159	159	6.275	0.981	1
X-1	35	34	3.518	0.831	1
C+X	174	174	5.890	0.971	1
C-2	48	48	4.564	0.906	1

It can be seen from Table 2 that the ACE and Chao indexes of sample C+X were both larger than that of sample C-1 and sample X-1. This is because the microbial communities in the BTF were abundant. Both chlorobenzene and xylene could be used as carbon source by bacteria, so the total number of species was relatively high. However, the Shannon and Simpson indexes of sample C+X were lower than those of sample C-1, but higher than those of sample X-1, which indicated that removal efficiency with chlorobenzene and xylene (Figure 6) was in accordance with the diversity and distribution of microbial species under a different carbon source. Meanwhile, all the α -diversification indexes (Table 2) of C-2 were higher than those of X-1. Therefore, it was speculated that an increase in the concentration of xylene not only inhibited the activity of chlorobenzene-degrading bacteria in the BTF, but reduced the diversity and distribution of chlorobenzene-degrading bacteria, leading to a decrease in the efficiency of removal of chlorobenzene.

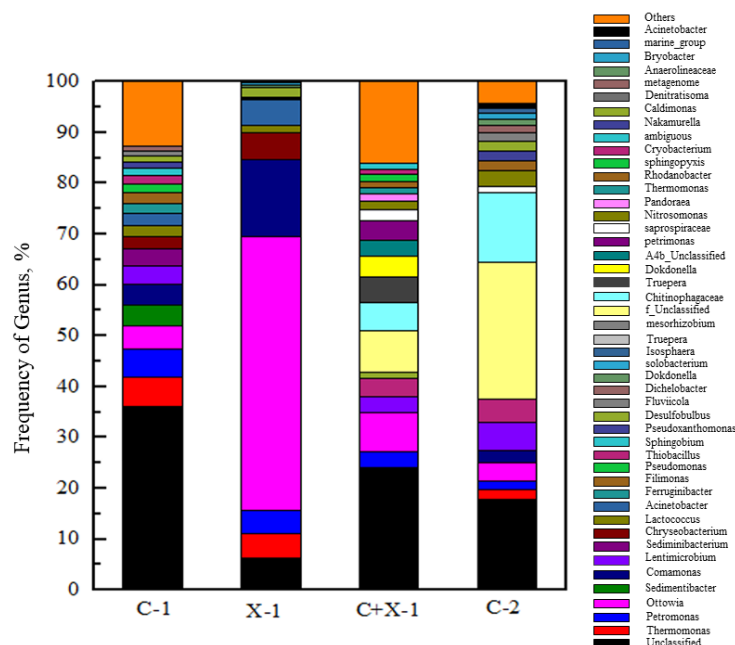
3.4.2. Analysis of the Microbial Communities

Table 3 shows the number of species at different classification levels for four different samples. It can be seen from Table 3 that the number of species in sample C-1 was greater than that of samples X-1 and C-2, indicating that the tolerance of chlorobenzene to microorganisms was greater than that of xylene. The abundance of species in sample C+X was greater than that of the other three sample, so it had enough microorganisms to effectively degrade chlorobenzene and xylene in the system. During the period of stable operation, the number of microbial species in the samples with only chlorobenzene under acid conditions was greater than that with xylene as the sole carbon source. It was also found that xylene is toxic to microorganisms.

Table 3. The number of species under different classification levels in each sample.

Sample	Phyla	Outline	Section	Family	Genera	Species
C-1	12	18	34	53	60	6
X-1	9	13	15	17	17	1
C+X	17	22	45	71	84	43
C-2	9	12	20	25	29	17

Figure 10 shows the distribution of the microbial communities of the four samples at genus level. It can be seen that the dominant flora was *Thermomonas* and *Petrimona* in the sample C-1; *Ottowia*, *Comamonas*, and *Chryseobacterium* in the sample C-2; *Ottowia* in the sample C+X, and *Lentimicrobium* in the sample C-2. *Thermomonas* and *Petrimona* accounted for 5.74% and 5.51% of the total amount of bacteria with chlorobenzene as the sole carbon source. Grabowski et al. [43] found that *Petrimonas* had strong ability to degrade complex organic compounds. Zhu et al. [44] found that *Thermomonas* could degrade aromatic compounds effectively under anaerobic condition. *Ottowia*, *Comamonas*, and *Chryseobacterium* accounted for 74.27% in total, and *Ottowia* accounted for 54.02% with xylene as the sole carbon source. Dafale et al. [45] observed that *Ottowia* was an aroma-degrading bacteria accumulated in UASB and SBR bioreactors. Compared with xylene as the sole carbon source, microorganisms in the system were much more abundant with mixed carbon sources. Under acid conditions with chlorobenzene as the sole carbon source, *Lentimicrobium*, which mainly treats high concentrations of organic compounds [46], accounted for 5.63%, while unnamed microorganisms accounted for a relatively high proportion of more than 50%. In general, the fluctuation of the operating conditions had a great impact on the microbial communities. Above all, the dominant bacteria in the system degrading chlorobenzene were *Thermomonas*, *Petrimona*, and *Comamona*, while the dominant bacteria degrading xylene was *Ottowia*.

**Figure 10.** The distribution of microbial communities at genus level.

4. Conclusions

This study revealed the key factors and corresponding gas–biomass kinetic mechanisms of chlorobenzene treatment from simulated flue waste gas in BTF. During the stable operation of the BTF, when an inlet concentration of chlorobenzene $700 \text{ mg}\cdot\text{m}^{-3}$, the oxygen concentration of 10%, and an EBRT of 80 s, the removal loading reached $38 \text{ g}\cdot\text{m}^{-3}\cdot\text{h}^{-1}$. The mass transfer kinetic analysis indicated that the process of chlorobenzene degrada-

tion in BTF was between the zero-stage reaction and the first-stage reaction. The BTF achieved a maximum biodegradability of chlorobenzene at an EBRT of 80 s under these experimental conditions. Therefore, the BTF appeared to achieve a higher biodegradability of chlorobenzene, overcoming the limitation of gas–liquid/solid mass transfer. The high-throughput sequencing results showed that *Thermomonas*, *Petrimona*, *Comana*, and *Ottowia* are typical organic-matter-degrading bacteria that degraded chlorobenzene efficiently with xylene present.

Author Contributions: Conceptualization, N.L.; methodology, J.-H.Z.; software, J.-L.L. and Y.-Y.Y.; validation, Y.-L.C. and J.-L.L.; formal analysis, K.Z. and Y.-L.C.; investigation, X.-Y.R. and Y.-Y.Y.; resources, J.-X.L. and J.-J.H.; data curation, J.-J.H. and N.L.; writing—original draft preparation, Y.-Y.Y. and Y.-L.C.; writing—review and editing, N.L. and J.-X.L.; supervision, C.M. and X.-Y.R. All authors have read and agreed to the published version of the manuscript.

Funding: This research was funded by National Key R&D Program of China grant number (2019YF E0122100), Key Science and Technology Program of Henan Province grant number (212102310514) and National Natural Science Foundation of China (51878646, 22131004 and 32071640).

Institutional Review Board Statement: Not applicable.

Informed Consent Statement: Not applicable.

Data Availability Statement: The data used to support the findings of this study are currently under embargo while the research findings are commercialized. Requests for data, 6 months after publication of this article, will be considered to upload to the repository of FIGSHARE.

Acknowledgments: The authors appreciate the support of the National Key R&D Program of China (2019YFE0122100); the Key Science and Technology Program of Henan Province (212102310514) and the National Natural Science Foundation of China (51878646, 22131004 and 32071640).

Conflicts of Interest: All of the authors declare that they have no conflict of interest.

Nomenclature

b	Rate constant of biodegradation
C_{in}	Inlet concentration of VOCs, $\text{mg}\cdot\text{m}^{-3}$
C_{out}	Outlet concentration of VOCs, $\text{mg}\cdot\text{m}^{-3}$
C_w	Concentration of contaminants in liquid/solid phase, $\text{mg}\cdot\text{m}^{-3}$
C_w^*	Concentration of contaminants in the liquid/solid phase at equilibrium, $\text{mg}\cdot\text{m}^{-3}$
D	Axial diffusion coefficient in gas phase
K	Transfer coefficient, h^{-1}
K_h	Ratio of pollutant concentration in liquid/solid phase and that in gas phase
K_m	Apparent semi-saturation constant, $\text{g}\cdot\text{m}^{-3}$
K_w	Ratio of pollutant mass in liquid/solid phase and that in gas phase
m_w	Henry coefficient of VOCs in liquid phase
n	The order of reaction
Q	Flue gas flow, $\text{m}^3\cdot\text{s}^{-1}$
q_e	Removal loading, $\text{g}\cdot\text{m}^{-3}\cdot\text{h}^{-1}$
r	Radius of BTF, m
R	Transfer rate of VOCs, $\text{mg}\cdot\text{m}^{-3}\cdot\text{s}^{-1}$
$[S]$	Concentration of the substrate, $\text{g}\cdot\text{m}^{-3}$
t_{EBRT}	Empty Bed Retention Time, s
t_R	Time of run, h
v	Interstitial velocity, $\text{g}\cdot\text{m}^{-3}\cdot\text{s}^{-1}$
V	Volume of the BTF, m^3
V_r	Effective volume of reactor, m^3
Z	Effective height of reactor, m
β_s^*	Maximum mass fraction of VOCs from gas to liquid phase
η	Removal efficiency with chlorobenzene, %
θ	Porosity of raschig-ring fillers
μ	Reduction rate, $\text{g}\cdot\text{m}^{-3}\cdot\text{s}^{-1}$
μ_{max}	Maximum apparent reduction rate, $\text{g}\cdot\text{m}^{-3}\cdot\text{s}^{-1}$

References

1. Boltic, Z.; Ruzic, N.; Jovanovic, M.; Savic, M.; Jovanovic, J.; Petrovic, S. Cleaner production aspects of tablet coating process in pharmaceutical industry: Problem of VOCs emission. *J. Clean. Prod.* **2013**, *44*, 123–132. [[CrossRef](#)]
2. Li, N.; Xing, X.; Cheng, J.; Zhang, Z.; Hao, Z. Influence of oxygen and water content on the formation of polychlorinated organic by-products from catalytic degradation of 1,2-dichlorobenzene over a Pd/ZSM-5 catalyst. *J. Hazard. Mater.* **2021**, *403*, 123952. [[CrossRef](#)]
3. Zhang, Y.; Liu, J.; Xing, H.; Li, J. Effect of liquid supply on the performance of a fungal bio-trickling filter treating hydrophobic VOC. *Biochem. Eng. J.* **2020**, *161*, 107658. [[CrossRef](#)]
4. Liu, D.; Andreasen, R.R.; Poulsen, T.G.; Feilberg, A. A comparative study of mass transfer coefficients of reduced volatile sulfur compounds for biotrickling filter packing materials. *Chem. Eng. J.* **2015**, *260*, 209–221. [[CrossRef](#)]
5. Coutu, C.; Martineau, G.; Guy, C.; Samson, R. Characterization of an organic filter medium for the bilofiltration treatment of air contaminated with 1, 2-dichlorobenzene. *J. Chem. Technol. Biotechnol.* **2003**, *78*, 907–917. [[CrossRef](#)]
6. Mathur, A.K.; Balomajumder, C. Performance evaluation and model analysis of BTEX contaminated air in corn-cob biofilter system. *Bioresour. Technol.* **2013**, *133*, 166–174. [[CrossRef](#)]
7. Caicedo, F.; Estrada, J.M.; Silva, J.P.; Muñoz, R.; Lebrero, R. Effect of packing material configuration and liquid recirculation rate on the performance of a biotrickling filter treating VOCs. *J. Chem. Technol. Biotechnol.* **2018**, *93*, 2299–2306. [[CrossRef](#)]
8. Zhang, Y.; Liu, J.; Xing, H.; Li, J. Performance and fungal diversity of bio-trickling filters packed with composite media of polydimethylsiloxane and foam ceramics for hydrophobic VOC removal. *Chemosphere* **2020**, *256*, 127093. [[CrossRef](#)]
9. Trellu, C.; Mousset, E.; Pechaud, Y.; Huguenot, D.; Hullebusch, E.D.; Esposito, G.; Oturan, M.A. Removal of hydrophobic organic pollutants from soil washing/flushing solutions: A critical review. *J. Hazard. Mater.* **2016**, *306*, 149–174. [[CrossRef](#)]
10. Guo, J.; Gao, Q. Enhancement of ethylbenzene removal from contaminated gas and corresponding mechanisms in biotrickling filters by a biosurfactant from piggery wastewater. *Environ. Manag.* **2021**, *277*, 111411. [[CrossRef](#)] [[PubMed](#)]
11. Rene, E.R.; Mohammad, B.T.; Veiga, M.C.; Kennes, C. Biodegradation of BTEX in a fungal biofilter: Influence of operational parameters, effect of shock-loads and substrate stratification. *Bioresour. Technol.* **2012**, *116*, 204–213. [[CrossRef](#)]
12. Zhang, L.; Zhang, C.; Cheng, Z.; Yao, Y.; Chen, J. Biodegradation of benzene, toluene, ethylbenzene, and o-xylene by the bacterium *Mycobacterium cosmeticum* byf-4. *Chemosphere* **2013**, *90*, 1340–1347. [[CrossRef](#)] [[PubMed](#)]
13. Li, K.; Zhou, J.; Wang, L.; Mao, Z.; Xu, R. The styrene purification performance of biotrickling filter with toluene-styrene acclimatization under acidic conditions. *J. Air Waste Manag. Assoc.* **2019**, *69*, 944–955. [[CrossRef](#)] [[PubMed](#)]
14. Blasi, B.; Poyntner, C.; Rudavsky, T.; Prenafeta-Boldú, F.X.; Hoog, S.D.; Tafer, H. Pathogenic yet environmentally friendly? black fungal candidates for bioremediation of pollutants. *Geomicrobiol. J.* **2015**, *33*, 308–317. [[CrossRef](#)] [[PubMed](#)]
15. Gallastegui, G.; Ramirez, A.Á.; Elías, A.; Jones, J.P.; Heitz, M. Performance and macrokinetic analysis of biofiltration of toluene and p-xylene mixtures in a conventional biofilter packed with inert material. *Bioresour. Technol.* **2011**, *102*, 7657–7665. [[CrossRef](#)]
16. Wang, X.; Wang, Q.; Li, S.; Li, W. Degradation pathway and kinetic analysis for p-xylene removal by a novel *Pandora* sp. strain WL1 and its application in a biotrickling filter. *J. Hazard. Mater.* **2015**, *288*, 17–24. [[CrossRef](#)] [[PubMed](#)]
17. Estrada, J.M.; Dudek, A.; Raul, M.; Guillermo, Q. Fundamental study on gas-liquid mass transfer in a biotrickling filter packed with polyurethane foam. *J. Chem. Technol. Biotechnol.* **2014**, *89*, 1419–1424. [[CrossRef](#)]
18. Yang, B.; Sun, Z.; Wang, L.; Li, Z.; Ding, C. Kinetic analysis and degradation pathway for m-dichlorobenzene removal by *Brevibacillus agri* DH-1 and its performance in a biotrickling filter. *Bioresour. Technol.* **2017**, *231*, 19–25. [[CrossRef](#)] [[PubMed](#)]
19. Liao, D.; Li, J.; Sun, D.; Xu, M.; An, T.; Sun, G. Treatment of volatile organic compounds from a typical waste printed circuit board dismantling workshop by a pilot-scale biotrickling filter. *Biotechnol. Bioprocess Eng.* **2015**, *20*, 766–774. [[CrossRef](#)]
20. Zhou, Q.; Zhang, L.; Chen, J.; Xu, B.; Chu, G.; Chen, J. Performance and microbial analysis of two different inocula for the removal of chlorobenzene in biotrickling filters. *Chem. Eng. J.* **2016**, *284*, 174–181. [[CrossRef](#)]
21. Kiernicka, J.; Seignez, C.; Peringer, P. *Escherichia hermannii*—A new bacterial strain for chlorobenzene degradation. *Lett. Appl. Microbiol.* **1999**, *28*, 27–30. [[CrossRef](#)]
22. Patel, T.A.; Vyas, K. Chlorobenzene degradation via Ortho-Cleavage Pathway by newly isolated *Microbacterium* sp. strain TAS1CB from a petrochemical-contaminated site. *Soil Sediment Contam.* **2015**, *24*, 786–795. [[CrossRef](#)]
23. Wang, X.; Lu, B.; Zhou, X.; Li, W. Evaluation of o-Xylene and other volatile organic compounds removal using a xylene-acclimated biotrickling filter. *Environ. Technol.* **2013**, *34*, 2691–2699. [[CrossRef](#)] [[PubMed](#)]
24. Bailón, L.; Nikolausz, M.; Kästner, M.; Veiga, M.C.; Kennes, C. Removal of dichloromethane from waste gases in one- and two-liquid-phase stirred tank bioreactors and biotrickling filters. *Water Res.* **2009**, *43*, 11–20. [[CrossRef](#)] [[PubMed](#)]
25. Wu, C.; Xu, P.; Li, W.; Li, S.; Wang, X.Q. o-Xylene removal using one- and two-phase partitioning biotrickling filters: Steady/transient-state performance and microbial community. *Environ. Technol.* **2017**, *27*, 6052–6065. [[CrossRef](#)] [[PubMed](#)]
26. Li, J.; Cai, W.; Zhu, L. The characteristics and enzyme activities of 4-chlorophenol biodegradation by *Fusarium* sp. *Bioresour. Technol.* **2011**, *102*, 2985–2989. [[CrossRef](#)] [[PubMed](#)]
27. Bordel, S.; Hernandez, M.; Villaverde, S.; Munoz, R. Modelling gas-liquid VOCs transport in two-liquid phase partitioning bioreactors. *Int. J. Heat Mass Transf.* **2010**, *53*, 1139–1145. [[CrossRef](#)]
28. Hernández, M.; Quijano, G.; Munoz, R.; Bordel, S. Modeling of VOC mass transfer in two-liquid phase stirred tank, biotrickling filter and airlift reactors. *Chem. Eng. J.* **2011**, *172*, 961–969. [[CrossRef](#)]

29. Drancourt, M.; Bollet, C.; Carlioz, A.; Martelin, R.; Gayral, J.P.; Raoult, D. 16S ribosomal DNA sequence analysis of a large collection of environmental and clinical unidentifiable bacterial isolates. *J. Clin. Microbiol.* **2000**, *38*, 3623–3630. [[CrossRef](#)]
30. Truelsen, D.; Pereira, V.; Phillips, C.; Morling, N.; Børsting, C. Evaluation of a custom GeneRead™ massively parallel sequencing assay with 210 ancestry informative SNPs using the Ion S5™ and MiSeq platforms. *Forensic Sci. Int. Genet.* **2021**, *50*, 102411. [[CrossRef](#)] [[PubMed](#)]
31. Wang, B.; Lu, L.; Zhang, Y.; Fang, K.; An, D.; Li, H. Removal of bisphenol A by waste zero-valent iron regulating microbial community in sequencing batch biofilm reactor. *Sci. Total Environ.* **2021**, *753*, 142073. [[CrossRef](#)]
32. Padhi, S.K.; Gokhale, S. Treatment of gaseous Yeoh, we hope we can keep it volatile organic compounds using a rotating biological filter. *Bioresour. Technol.* **2017**, *244*, 270–280. [[CrossRef](#)] [[PubMed](#)]
33. Wei, Z.; Li, H.; He, J.; Ye, Q.; Huang, Q.; Luo, Y. Removal of dimethyl sulfide by the combination of non-thermal plasma and biological process. *Bioresour. Technol.* **2013**, *146*, 451–456. [[CrossRef](#)] [[PubMed](#)]
34. Lebrero, R.; Rodriguez, E.; Estrada, J.M.; Garcia-Encina, P.A.; Munoz, R. Odor abatement in biotrickling filters: Effect of the EBRT on methyl mercaptan and hydrophobic VOCs removal. *Bioresour. Technol.* **2012**, *109*, 38–45. [[CrossRef](#)]
35. Popat, S.C.; Zhao, K.; Deshusses, M.A. Bioaugmentation of an anaerobic biotrickling filter for enhanced conversion of trichloroethene to ethene. *Chem. Eng. J.* **2012**, *183*, 98–103. [[CrossRef](#)]
36. Li, Z.X.; Yang, B.R.; Jin, J.X.; Pu, Y.C.; Ding, C. The operating performance of a biotrickling filter with *Lysinibacillus fusiformis* for the removal of high-loading gaseous chlorobenzene. *Biotechnol. Lett.* **2014**, *36*, 1971–1979. [[CrossRef](#)]
37. Yang, B.; Li, Y.; Shang, Q.; Ding, C.; Xu, Q. Biodegradation of *o*-dichlorobenzene by *Bacillus cereus* DL-1: Kinetics, degradation pathway, biodegradability and performance in biotrickling filter. *Environ. Pollut. Bioavail.* **2020**, *32*, 79–86. [[CrossRef](#)]
38. Xu, P.; Wei, Y.; Ma, C.; Li, S.; Guo, T.; Wang, X.; Li, W. Multi-factorial analysis of the removal of dichloromethane and toluene in an airlift packing bioreactor. *J. Environ. Manag.* **2020**, *261*, 109665. [[CrossRef](#)]
39. Dobslaw, D.; Schöller, J.; Krivak, D.; Helbich, S.; Engesser, K.H. Performance of different biological waste air purification processes in treatment of a waste gas mix containing tert-butyl alcohol and acetone: A comparative study. *Chem. Eng. J.* **2019**, *355*, 572–585. [[CrossRef](#)]
40. Jiang, X.; Yan, R.; Tay, J.H. Simultaneous autotrophic biodegradation of H₂S and NH₃ in a biotrickling filter. *Chemosphere* **2009**, *75*, 1350–1355. [[CrossRef](#)]
41. Chen, Y.; Fan, Z.; Ma, L.; Yin, J.; Luo, M.; Cai, W. Performance of three pilot-scale immobilized-cell biotrickling filters for removal of hydrogen sulfide from a contaminated air stream. *Audi J. Biol. Sci.* **2014**, *21*, 450–456. [[CrossRef](#)] [[PubMed](#)]
42. Xie, L.; Zhu, J.; Hu, J.; Jiang, C. Study of the mass transfer-biodegradation kinetics in a pilot-scale biotrickling filter for the removal of H₂S. *Ind. Eng. Chem. Res.* **2020**, *59*, 8383–8392. [[CrossRef](#)]
43. Grabowski, A.; Tindall, B.J.; Bardin, V.; Blanchet, D.; Jeanthon, C. *Petrimonas sulfuriphila* gen. nov., sp. nov., a mesophilic fermentative bacterium isolated from a biodegraded oil reservoir. *Int. J. Syst. Evol. Microbiol.* **2005**, *55*, 1113–1121. [[CrossRef](#)]
44. Zhu, Y.; Wang, W.; Ni, J.; Hu, B. Cultivation of granules containing anaerobic decolorization and aerobic degradation cultures for the complete mineralization of azo dyes in wastewater. *Chemosphere* **2020**, *246*, 125753. [[CrossRef](#)]
45. Dafale, N.; Agrawal, L.; Kapley, A.; Meshram, S.; Purohit, H.; Wate, S. Selection of indicator bacteria based on screening of 16S rDNA metagenomic library from a two-stage anoxic-oxic bioreactor system degrading azo dyes. *Bioresour. Technol.* **2010**, *101*, 476–484. [[CrossRef](#)]
46. Wang, H.; Chen, N.; Feng, C.; Deng, Y.; Gao, Y. Research on efficient denitrification system based on banana peel waste in sequencing batch reactors: Performance, microbial behavior and dissolved organic matter evolution. *Chemosphere* **2020**, *253*, 126693. [[CrossRef](#)] [[PubMed](#)]